J Mol Model (2013) 19:4305–4318
DOI 10.1007/s00894-013-1944-3

ORIGINAL PAPER

Structure-based approach to the design of BakBH3 mimetic peptides with increased helical propensity

Laura Delgado-Soler · Maria del Mar Orzaez · Jaime Rubio-Martinez

Received: 30 March 2013 / Accepted: 11 July 2013 / Published online: 31 July 2013
© Springer-Verlag Berlin Heidelberg 2013

Abstract The Bcl-2 family of proteins are well-characterized regulators of the intrinsic apoptotic pathway. Proteins within this family can be classified as either prosurvival or prodeath members and the balance between them present at the mitochondrial membrane is what determines if the cell lives or dies. Specific interactions among Bcl-2 family proteins play a crucial role in regulating programmed cell death. Structural studies have established a conserved interaction pattern among Bcl-2 family members. This interaction is mediated by the binding of the hydrophobic face of the amphipathic α-helical BH3 domain into a conserved hydrophobic groove on the prosurvival partners. It has been reported that an increase in the helical content of BH3 mimetic peptides considerably improves the binding affinity. In this context, this work states for designing peptides derived from the BH3 domain of the proapoptotic protein Bak by substitution of some non-interacting residues by the helical inducing residue Aib. Different synthetic peptides preserving BakBH3 relevant interactions were proposed and simulated presenting a better predicted binding energy and higher helical content than the wild type Bak peptide.

Keywords Aib · Apoptosis · Bcl-x_L · Drug design · Helicity · Molecular dynamics

Introduction

Tumoural processes are often characterized by an evasion of cellular apoptotic pathways which are controlled by the balance between endogenous propapototic molecules and endogenous apoptosis inhibitors [1, 2].

Two major signaling cascades lead to cell death: the extrinsic and the intrinsic pathways [3, 4]. The former involves the activation of caspase proteases by receptors placed on the cell surface whereas in the later, caspases are activated by an apoptosome that is assembled after the release of several pro-apoptotic factors, including cytochrome c, from the mitochondrion. Indeed, mitochondrial outer membrane permeabilization is considered an irreversible step in committing a cell to apoptosis.

The Bcl-2 family proteins are well-characterized regulators of the intrinsic apoptotic pathway [3, 5–7]. Proteins within this family can be classified either as prosurvival or as prodeath members and is the balance between them present at the mitochondrial membrane that determines cell death or survival.

Specific interactions among Bcl-2 family proteins play a crucial role in the regulation of programmed cell death. These protein–protein interactions are mediated by regions of highly conserved sequences known as Bcl-2 homology (BH) domains, of which there are four, BH1 to BH4 [8]. Bcl-2 proteins can be distinguished by their structural features and can be grouped into three subfamilies based on the number of these BH domains they share [9]. The first subfamily has the four domains (BH1-4) and includes the anti-apoptotic proteins Bcl-2, Bcl-x_L, Bcl-w, Mcl-1 and Bfl-1. The next two groups are proapoptotic proteins possessing three BH (BH1–3) domains represented by Bax, Bak and Bok, and BH3-only proteins, such as Bim, Bid, Bad, Puma, Noxa, Hrk, and Bmf, which are

Electronic supplementary material The online version of this article (doi:10.1007/s00894-013-1944-3) contains supplementary material, which is available to authorized users.

L. Delgado-Soler · J. Rubio-Martinez (✉)
Department of Physical Chemistry, University of Barcelona (UB) and Institut de Química Teòrica i Computacional (IQTCUB), Universitat de Barcelona, C/Martí i Franquès 1, 08028 Barcelona, Spain
e-mail: jaime.rubio@ub.edu

M. del Mar Orzaez
Department of Medicinal Chemistry, Centro de Investigación Príncipe Felipe, Valencia, Spain

M. del Mar Orzaez
Instituto de Biomedicina de Valencia, CSIC, Valencia, Spain

characterized by the presence of a single BH domain (as their name implies, the BH3 domain).

Structural studies have established a conserved interaction mode among Bcl-2 family members. This interaction is governed by the binding of the hydrophobic face of the amphipathic α-helical BH3 region of the proteins into a conserved hydrophobic groove on the prosurvival proteins formed by the BH1, BH2, and BH3 domains of prosurvival proteins [10, 11]. This interaction geometry is shared by BH3 regions from both BH3-only and multidomain proapoptotic proteins, even by Bcl-2 family members of low sequence similarity.

Some available experimental results support the idea that intermolecular interactions established between these domains alone are not always enough to explain experimental binding affinities. In fact, after analyzing the ability of different BaxBH3 peptide variants to inhibit the heterodimerization of wild-type Bax with Bcl-2 and Bcl-XL, Shangary et al. concluded that high helical content correlated with peptide activity despite not being sufficient [12].

Besides, it has also been suggested that the addition of some N-terminal and C-terminal fragments to the BH3 domain core induced a substantial increase in their binding affinity. This fact is not attributed to an increase of the interacting residues but to a stabilization of the helical conformation of bioactive peptide [13, 14].

Bearing in mind this idea, different approaches have been devised to increase the helical propensity of BH3 peptides. As previously commented, Liu et al. [13], added N- and C-terminal segments of five residues, extracted from the terminal regions of the Bad_{25}BH3 peptide, to X_{16}BH3 peptides derived from Bak, Bax and Bid to induce a substantial increase in its Bcl-2-binding affinity by stabilizing its helical structures.

Thus, it seems that intramolecular interactions that favor bioactive peptide conformation could be determinant for peptide activity, as in the case of peptides bonded in a helical conformation. Accordingly, Yang et al. [15] incorporated a lactam bridge to generate highly helical Bak_{16}BH3 peptides. However, none of the synthesized peptides showed inhibitory activity against Bcl-2, probably because the introduction of steric hindrance with the receptor.

A better understanding of these complex effects can be achieved by computational techniques, revealing the dynamic behavior of the protein complexes with natural or suggested synthetic peptides. Conformational space explored by peptides and the relative contributions of different energetic terms to complex formation can be analyzed and later on, correlated with experimentally determined binding affinities.

Different theoretical studies have described the relationship between helix stability and binding affinity of pro-apoptotic BH3 peptides to some anti-apoptotic Bcl-2 protein family members [16–18].

The alpha-aminoisobutyric (Aib) non-natural aminoacid has generally been considered to be a strongly helicogenic residue as evidenced by its ability to promote helical folding in synthetic and natural sequences [19–21]. Thus, replacing non-interacting residues of the BH3 domains by Aib residues appears as an appealing strategy for increased peptide binding affinities.

If helical propensity plays an important role in the interaction of BH3-derived peptides of proapoptotic proteins with their antiapoptotic binding partners, molecular dynamics studies should be performed using a force field that properly describes its helical features. In order to better understand the helical properties of the different studied complexes, three widely used force fields have been used in this work. The first one is the ff94 [22] force field of the AMBER package [23, 24] for which a tendency to favor helical structures in decrement of the turns and sheets structures in long molecular dynamics has been reported [25]. With the goal to provide an improved balance between extended and helical conformations, Hornak et al. performed a throughout reparametrization of backbone torsional terms using alanine and glycine tetrapeptides [26] that was included in the ff99SB parameterization. Finally, ff03 force field developed by Duan et al. [27] represents a new approach to the development of parameters in the context of the AMBER package.

The goal of the present work is to obtain BakBH3 derived peptides with an enhanced affinity for the Bcl-XL protein. For this purpose, computational techniques are used to study the wild type Bak peptide complex and to determine relevant interactions involved in the binding process. Later on, synthetic peptides are proposed by replacing non-contributing Bak residues by Aib residues in order to increase helical propensity of the BH3 domain of these peptides. The aim is to design new BH3-based peptides with an increased affinity for the Bcl-x_L protein. Theoretical calculations will be used to estimate binding energies and describe helical structures characteristic of these complexes.

Computational methods

Simulation setup

Starting structure for the molecular dynamics study of the natural Bak_{16} peptide was directly obtained from experimental NMR structure of its complex with the Bcl-x_L protein (entry 1BXL of the Protein Data Bank) [28]. Different synthetic peptides were proposed substituting non-interacting Bak residues with the Aib aminoacid (see Table 1). Mutations on terminal positions were omitted to avoid possible synthetic problems. As glycine in 11th position has been reported to be determinant for peptide binding, for each peptide sequence two variants were analyzed, one preserving the Gly in this position and a second mutating this residue to Aib. Different peptides were also suggested removing some non-interacting

Table 1 Sequence of the different Bak-derived peptides analyzed

Peptides	Residue position															
	1	2	3	4	5	6	7	8	9	10	11	12	13	14	15	16
Bak	G	Q	V	G	R	Q	L	A	I	I	G	D	D	I	N	R
$Bak_{16}Aib_4$	G	Q	V	Aib	R	Aib	L	Aib	I	I	Aib	D	D	I	N	R
$Bak_{16}Aib_3G$	G	Q	V	Aib	R	Aib	L	Aib	I	I	G	D	D	I	N	R
$Bak_{16}Aib_6$	G	Aib	V	Aib	R	Aib	L	Aib	I	I	Aib	D	D	I	Aib	R
$Bak_{16}Aib_5G$	G	Aib	V	Aib	R	Aib	L	Aib	I	I	G	D	D	I	Aib	R
$Bak_{14}Aib_5$	–	–	V	Aib	R	Aib	L	Aib	I	I	Aib	D	D	I	Aib	R
$Bak_{14}Aib_4G$	–	–	V	Aib	R	Aib	L	Aib	I	I	G	D	D	I	Aib	R
$Bak_{14}Aib_4$	–	Q	V	Aib	R	Aib	L	Aib	I	I	Aib	D	D	I	N	–
$Bak_{14}Aib_3G$	–	Q	V	Aib	R	Aib	L	Aib	I	I	G	D	D	I	N	–
$Bak_{13}Aib_4$	–	–	V	Aib	R	Aib	L	Aib	I	I	Aib	D	D	I	N	–
$Bak_{13}Aib_3G$	–	–	V	Aib	R	Aib	L	Aib	I	I	G	D	D	I	N	–

terminal residues. Finally, a set of 11 peptides $Bak_xAib_yG_z$ was obtained, where x stands for the total length of each peptide, y corresponds to the number of positions replaced by Aib and z (which can be 1 or 0) indicates the presence or not of the glycine on 11th position.

Structures for the complexes with synthetic peptides were also generated from the same experimental structure but retaining only the coordinates of the backbone atoms for mutated positions and the non-modified residues of the Bak hexadecapeptide. Finally, for the wild type BakBH3 and the three best predicted candidates, structures for the free peptides were also considered for further analysis. Then, side chains for the Aib aminoacids were added using the *LEaP* module of the AMBER9 suite [23, 24].

Next, an identical protocol was followed for all complexes. Structures were neutralized with counterions, following a grid-shaped procedure for mapping electrostatic potential surface. Finally, a cubic box of TIP3P waters [29] was created within a minimum distance between the protein and the edge of the box of 15 Å and removing water molecules closer than 2.2 Å to any of the protein atoms.

All calculations for the complexes were carried out at the molecular mechanics level using three different amber force fields: ff94 [22], ff99SB [26] and ff03 [27]. For the free peptides, only ff99SB was considered due to structural incongruences observed in the complexes analysis for the remaining force field parameterizations. Parameters for the Aib aminoacid were obtained from Bisetty et al. [30]

Molecular dynamics simulations

Bad contacts derived from the addition of the new sidechains should be removed to achieve a proper starting structure to perform molecular dynamics studies. Thus, systems were energy-minimized using the steepest descent algorithm. Four steps of 10.000 iterations were performed allowing only a partial system optimization restraining the other movement with harmonic potential penalties. First, only water and counterion molecules were minimized. In the second stage, sidechains of the X_{16} peptides were included in the optimization. Then, receptor sidechains were also relaxed and in the last minimization stage, a free receptor is considered. Finally, 10.000 iterations were calculated with the whole system free.

Molecular dynamics of the complexes were performed at a constant temperature of 300 K by coupling the systems to a thermal bath using Berendsen's algorithm [31] with a time coupling constant of 0.2 ps. Long-range electrostatic energy was computed using the Particle Mesh Ewald summation method [32]. SHAKE algorithm [33] was used to constrain the bonds involving the hydrogen atoms and to allow an integration time of 2 fs. The minimized structures were heated at 300 K at a constant rate of 30 K/10 ps with harmonic restrains in protein atoms. Once the systems were heated, two steps of 20 ps at constant pressure were performed to increase the system density and to gradually remove restrains. A temperature coupling constant of 1.0 ps and 2.0 ps. was applied during the first and second steps respectively. Finally, molecular dynamics of length between 35 and 45 ns were calculated within the NVT ensemble for each of the 11 considered complexes. To include the higher peptide mobility, 100 ns molecular dynamics simulations were considered for free peptide systems taking as starting structures those extracted from minimized complexes.

MMPB/GBSA calculations

The molecular mechanics Poisson Boltzmann/generalized Born surface area approach (known as MMPB/GBSA) is

one of the most widely used methods to estimate protein-ligand binding free energies [34, 35]. By using a thermodynamic path (depicted in Fig. 1) that includes the solvation contributions, the following expression is obtained:

$$\Delta G_b = \Delta G_b^0 + \Delta G_C^{0\to sol} - \Delta G_R^{0\to sol} - \Delta G_L^{0\to sol} = \Delta G_b^0 + \Delta G^{sol}$$

where ΔG_b^0 accounts for the free energy of binding in vacuo and ΔG^{sol} is the difference between the solvatation free energy of the receptor-ligand complex (C) and the sum of the solvatation free energy of the free receptor (R) and ligand (L).

The binding free energy in vacuo can be decomposed itself into enthalpic and entropic contributions as:

$$\Delta G_b^0 = \Delta H_b^0 - T\Delta S_b^0$$

Assuming that system volume change is negligible upon ligand binding, the enthalpic term can be computed by molecular mechanics. Then it can be expressed as a sum of strain energies from covalent bonds and torsion angles as well as non-covalent van der Waals and electrostatic energies. Thus:

$$\Delta H_b^0 \approx \Delta E_{MM} = \Delta E_{bond} + \Delta E_{angle} + \Delta E_{torsion} + \Delta E_{vdW} + \Delta E_{elec}$$

These energetic values are determined with the *sander* program from AMBER9 suite. No cutoff is considered for all calculations.

The solvation terms (ΔG^{sol}) are decomposed into a sum of electrostatic (or polar) and non-polar contributions:

$$\Delta G^{sol} = \Delta G_{pol}^{sol} + \Delta G_{np}^{sol}$$

The electrostatic contribution can be computed using a numerical solver for the Poisson-Boltzmann equation (PB), as implemented in the *pbsa* program [36] from AMBER9 suite [37, 38] or estimated by means of generalized Born (GB) methods. Tsui and Case GB parameters [39] were used in this work.

In the present work, the nonpolar contribution was computed with the LCPO method [40] where non polar salvation energy is estimated from the change in the solvent accessible surface area (SASA) [41] as:

$$\Delta G_{np}^{sol} = \gamma \quad \Delta(SASA) + \beta$$

with γ=0.00542 *kcal* (*mol* Å^2)$^{-1}$ and β=0.92 *kcal mol*$^{-1}$, when using the PB method or by:

$$\Delta G_{np}^{sol} = \gamma \quad \Delta(SASA)$$

with γ=0.005 *kcal* (*mol* Å^2)$^{-1}$, when using the GB approach.

In this work a one-trajectory protocol is used which means that the set of complex conformations extracted can be used to generate a separate set of structures for the unbound receptor and ligand. This approximation avoids the calculation of separated trajectories free receptor and ligands but it can be only applied when small conformational changes take place during ligand binding. However, this approximation can be useful in order to compare different methodologies to compute binding energies where conformational changes cannot be taken into account.

To have a representative measure of the binding free energy, MMPB/GBSA energies were calculated for structures extracted every 10 ps of the whole molecular dynamics trajectory. Mean values were calculated for 5 ns intervals in order to determine if convergence has been achieved for binding energies.

In order to determine relevant Bak aminoacids, the contribution of each residue to the binding free energy was estimated using the MM-GB/SA per residue protocol [42]. This approach considers that all pairwise interactions are equally distributed between interacting atoms. Thus, each residue contribution is computed as the sum of its interactions in vacuo and the corresponding solvation contribution.

For the most stable peptides studied, the entropic contribution was obtained as an average over 100 snapshots extracted at a time interval of 10 ps from the last 1 ns of each ff99SB trajectory using the normal mode analysis within the harmonic approximation.

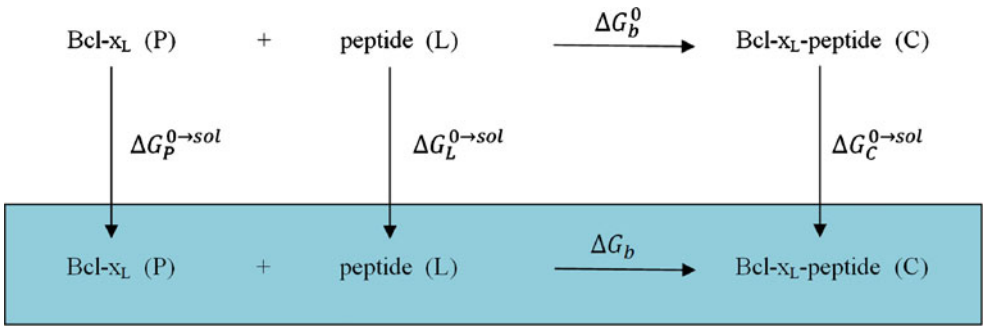

Fig. 1 Thermodynamic cycle used in the MMPB/GBSA methodology to obtain binding the free energy (ΔG_b) from the binding free energy in vacuo (ΔG_b^0) and solvatation free energies ($\Delta G^{0->sol}$)

Hydrogen-bond interactions

Hydrogen bonds between Bak peptide and Bcl-x_L protein were determined using the *ptraj* module of the AMBER suite. Hydrogen bond donor and acceptor atoms were defined for each protein residue and next, distances and angles between potential hydrogen bonded atoms were analyzed for snapshots obtained every 10 ps of the molecular dynamics trajectory. The criteria considered for H-bonding was a distance between donor and acceptor atoms under 3.5 Å, an acceptor–H-donor angle (Θ_{HB}) of more than 120° and a lifetime higher than the 30 % of the total number of snapshots analyzed. Values for the hydrogen bond angles are reported as 180 - Θ_{HB}, as calculated in AMBER v9.

Helical content analysis of peptide residues

As binding affinity for the Bcl-2 protein family has been often related to peptides helicity, the secondary structure for the most potent inhibitory peptides was analyzed using the DSSP algorithm of Kabsch and Sander [43]. To extract representative conformations, the whole molecular dynamics trajectories for complexes and free peptides were considered. Snapshots were obtained every 10 or 20 ps for complexes and peptide simulations, respectively.

Accordingly, to quantify and compare helical properties of different peptides, averaged helical properties such as helical propensity, helix ratio and residue length in a helical segment were computed for the final interval of molecular dynamics trajectories. To include a representative conformational analysis, only the final 5 ns were considered for complex dynamics whereas for free peptide simulations this analysis was extended to the last 25 ns due to their higher mobility. Helical propensity for a given residue is computed as the ratio between the number of snapshots where it is predicted to be in a helical conformation and the total number of snapshots analyzed. Helix ratio is defined as the number of residues in helical segments divided by the total number of residues in the peptide. Finally, residue length is defined as the occurrence of a given helix length in all helical segments.

Results and discussion

Interaction analysis of the Bak/Bcl-x_L complex

The first step for designing new Bak-derived peptides with high affinity for the Bcl-x_L protein goes through determining residues involved in wild type peptide binding. For this purpose, molecular dynamics simulations were performed starting from the NMR structure of the wild type Bak/Bcl-x_L complex, using three different widely used force fields. Later on, significant interactions obtained from different force field simulations were analyzed to extract reliable conclusions about Bak binding pattern.

Starting point for molecular dynamics is an experimentally determined structure, no significant differences were expected in conformational space explored by the bound peptide within the three force field simulations. However, when superimposing NMR coordinates with final molecular dynamics structures some differences are observed in peptide position. The C-terminal residues of the Bcl-x_L protein constitute a mobile region which in principle should be interacting with some Bak nearby residues. Depending on the parameterization used this region moves inducing some conformational changes in the peptide to preserve these interactions (see Fig. 2). In the ff94 and ff99SB parameterization, final residues practically preserve the NMR position. Thus, peptide position is completely equivalent to that observed on the NMR

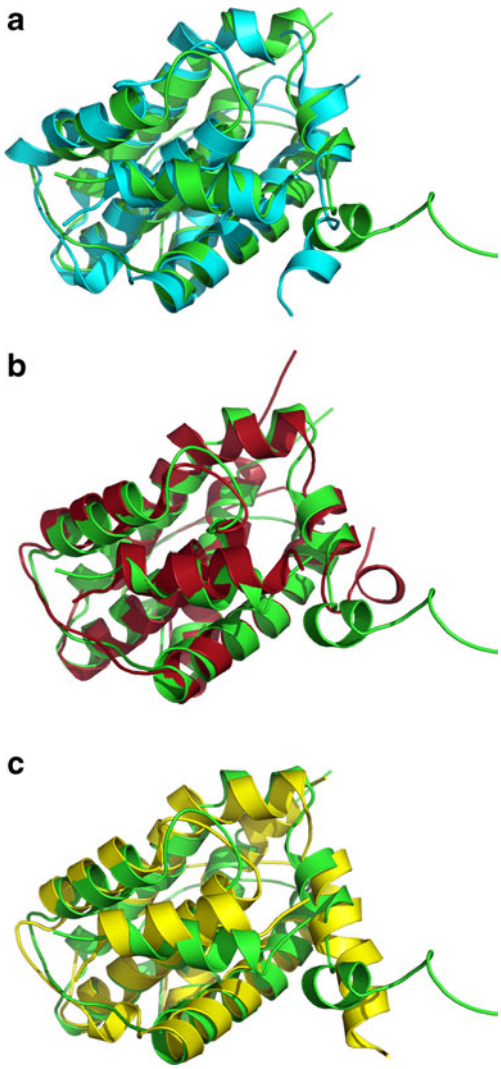

Fig. 2 Superposition of final structures from molecular dynamics simulations with the experimentally determined X-ray structure (*in green*) for **a**) ff94 force field trajectory (*in blue*); **b**) ff99SB trajectory (*in red*); and **c**) ff03 trajectory (*in yellow*)

structure. Conversely, ff03 induces a helical conformation of these C-terminal residues that also supposes a displacement on peptide position.

Accordingly, different peptide positions lead to different interactions with receptor. Thus, as discussed below, some differences appeared in the interaction analysis depending on the force field parameterization used (see Table 2 for hydrogen bonds and Table 3 for binding free energy values).

Typical hydrophobic interactions of the Bcl-2 protein family binders [14, 44] were found in all three simulations (see Table S1b). Accordingly, four significant vdW interactions span over the binding groove corresponding to residues which are occupying the four hydrophobic pockets (h1 to h4). Interacting residues obtained from the ff94 and ff99SB simulations completely agree with experimentally relevant vdW residues: Val74, Leu78, Ile81 and Ile85 occupying the pockets h1 to h4, respectively [28]. However, despite ff03 force field also seems to present the four hydrophobic contacts, the most important contributions to the binding come from different residues (Gln73, Gln77, Ile80 and Asp84) which are occupying the hydrophobic pockets instead of the known experimental residues which cannot achieve their optimal interactions due to the previously discussed peptide displacement. When focusing on electrostatic interactions (see Table S1c), some discrepancies were also found within the three used force fields. Omitting interactions derived from terminal residues, again ff94 and ff99SB predict experimentally determined interactions [28]. Indeed, a favorable electrostatic contribution for Arg76 was predicted, unfavorable interactions for Asp83 and Asp84, although to a lesser extent for the latter. Significant contributions have been determined experimentally for Arg76 and Asp83. The former, is in good agreement with favorable ΔG values predicted for this residue (which also have an important hydrophobic contribution) but the latter remains unexplained. Unfavorable contributions of Asp83 and Asp84 are completely counteracted by solvation effects and their contribution to the binding energy is practically negligible (Table S1a). However, no favorable contribution is predicted for Asp83 to explain significance observed experimentally. Thus, the effect observed for this residue may be attributed to intramolecular interactions that stabilize bioactive conformation. When considering the ff03 parameterization, surprising results were found for the most important electrostatic contributions. Interactions observed in this case do not correspond with typical interacting polar residues. In fact, two significant electrostatic contacts were predicted for the ff03 parameterization, both corresponding to glycine residues, concretely Gly75 and Gly82 with favorable and unfavorable contributions, respectively. Asp83 also has an important unfavorable contribution, as observed for the former force fields. However, all these electrostatic contributions are again cancelled by solvation energies. Thus, the only significant electrostatic contribution observed for Arg76 is not present in the ff03 simulation due to peptide displacement, as other electrostatic interactions observed appear counteracted by solvation effects.

Concerning the hydrogen bonding pattern (Table 2), two hydrogen bonds were determined for ff94 and ff99SB force

Table 2 Hydrogen bonds determined between the Bak peptide and the Bcl-x_L protein for the ff94, ff03 and ff99SB simulations

	Bcl-x_L	Bak	Occupancy (%)	Distance (Å)	Angle (º)
ff94	GLU 129 OE2	ARG 76 HE-NE	47.6	2.81±0.11	24.2±10.7
	GLU 129 OE1	ARG 76 HE-NE	46.2	2.84±0.14	25.6±11.0
	GLU 129 OE2	ARG 76 HE-NE	34.4	3.10±0.23	42.4±9.2
	ARG 100 HH21-NH2	ASP 84 OD2	73.4	2.82±0.16	29.9±11.2
	ARG 100 HE-NE	ASP 84 OD2	69.8	2.93±0.20	32.6±10.5
	ARG 100 HH21-NH2	ASP 84 OD1	38.4	2.90±0.23	29.1±11.5
ff03	GLU 129 OE1	ARG 76 HH21-NH2	32.6	2.87±0.11	28.6±11.6
	GLN 111 HE21- NE2	GLN 77 OE1	88.4	2.96±0.17	28.6±12.7
	ARG 139 HE - NE	ALA 79 O	39.8	3.01±0.18	24.5±11.7
	ARG 100 HH21-NH2	ASP 84 OD1	36.8	2.92±0.21	26.7±11.7
	LEU 194 O	ARG 87 HH21 – NH2	30.2	2.89±0.15	24.6±11.5
ff99SB	GLU 129 OE2	ARG 76 HH21-NH2	59.2	2.91±0.22	31.9±10.6
	GLU 129 OE2	ARG 76 HE-NE	52.2	2.93±0.19	31.0±10.2
	GLU 129 OE1	ARG 76 HH21-NH2	44.8	2.93±0.21	32.3±12.3
	GLU 129 OE1	ARG 76 HE-NE	38.4	2.96±0.20	30.3±11.2
	ARG 100 HH21-NH2	ASP 84 OD1	83.6	2.81±0.12	22.1±10.7
	ARG 100 HE-NE	ASP 84 OD1	39.6	3.07±0.21	37.1±9.3
	TRP 137 O	ASN 86 HD21 - ND2	79.2	2.98±0.16	18.7±10.3

Table 3 Free energy decomposition analysis of Bak peptide: residues remarked in green correspond with favorable van der Waals interactions (< −4 kcal mol^{-1}) whereas blue and red residues correspond with favorable (< −50 kcal mol^{-1}) and unfavorable (> 50 kcal mol^{-1}) electrostatic interactions, respectively. Hydrogen bonded residues of the Bcl-x_L protein are also shown

	G72	Q73	V74	G75	R76	Q77	L78	A79	I80	I81	G82	D83	D84	I85	N86	R87
ff94					E129								R100			
ff99SB					E129								R100		W137	
ff03						Q111										

fields: Arg76 and Asp84 interacting with Glu129 and Arg100 of Bcl-x_L, respectively. The only difference between ff94 and ff99SB force field is an extra hydrogen bond established in the ff99SB simulation (between Asn86 of Bak peptide and Trp137 of the Bcl-x_L protein) that has been lost in the ff94 simulation (Asn86 is solvent oriented). For the ff03, these H-bonds cannot be achieved and a single hydrogen bond between residue Gln77 and Gln111 of Bcl-x_L protein was found. Despite not appearing in the other simulations, Gln77 also have the proper orientation to be hydrogen bonded to Gln111 in all three simulations as well as in the NMR structure.

Free energy decomposition accounts for hydrophobic and electrostatic contributions discussed above but also takes into account the solvation effects. Similar behavior is observed for ff94 and ff99SB force fields even at quantitative level. However, as previously discussed for peptide interactions, significant contributions observed for the ff03 force field are completely different. MMGBSA per residue values can be found in Fig. S1 of supporting information.

In conclusion, it can be said that ff94 and ff99SB predict an equivalent binding pattern for the wild type Bak peptide. Moreover, relevant residues determined by interaction analysis completely agree with experimentally well-known interacting residues [28]. Oppositely, ff03 parameterization does not seem to reproduce experimental results. Despite the four typical hydrophobic pockets seem to be occupied in the interaction analysis, relevant Bak residues are displaced in comparison with experimental ones. The same occurs with electrostatic interactions. Therefore, only results derived from the ff94 and ff99SB parameterizations should be taken into consideration for further calculations.

MMPB/GBSA convergence

Different peptides were proposed by replacement of the previously determined non-interacting Bak residues by the non-natural Aib aminoacid. Then, molecular dynamics of length at least 35 ns of the $Bak_xAib_yG_z$-Bcl-x_L complexes were carried out. MMPB/GBSA methodology was used to estimate binding affinity of these new peptides for the Bcl-x_L protein.

Initial structures for synthetic peptides complexes were directly obtained by homology modeling of Bak NMR coordinates. Hence, in order to determine if convergence has been achieved and thus, predict reliable ΔG values, binding free energies were averaged for every 5 ns of the whole molecular dynamics trajectories (see Tables S.2 to S.7 of supporting information).

According to discrepancies observed for the ff03 force field and available experimental data, only ff94 force field was used to select a first set of synthetic peptides, as equivalent results can be expected from the ff99SB parameterization. Considering the overall of binding free energy values obtained along the first 35 ns of molecular dynamics trajectories (see Table 4 and more detail is provided on Tables S.2 to S.7 of supporting information), all peptides with predicted binding affinity for the Bcl-x_L protein at least 5 kcal mol^{-1} greater than the wild type Bak were initially retained. However, an exception was made concerning $Bak_{13}Aib_3G$ peptide also being retained for further analysis. Despite having a mean binding free energy smaller than cutoff considered, a decrease of binding free energy was observed during the last 10 ns presenting this peptide as a potential candidate after ΔG stabilization. Later on, ff94 and ff99SB were used to simulate and score the peptides with the higher predicted binding affinity. For the selected peptides, molecular dynamics simulations were extended 5 ns to ensure that the convergence of binding free energy values has been achieved. Even though, dynamics and binding free energies were also calculated using the ff03 parameterization as an additional score for evaluating these peptides.

When focusing on the ff03 results, only one of the proposed peptides was predicted to overcome wild type Bak binding affinity for the Bcl-x_L protein. The remaining peptides were not expected to exhibit an improved efficiency according to their estimated binding free energies. These poor affinities predicted for ff03 simulations can be attributed to the fact that peptide mutations were based only on ff94 and ff99SB relevant interactions. Thus, important residues according to ff03 parameterization may have been replaced by Aib and those interactions lost, leading to low binding free energy values. Thus, ff03 predicted binding free energies cannot be taken into account for peptide selection

Accordingly, MMPB/GBSA values within the last 10 ns (see Table 4) for the ff94 and ff99SB simulations were used to

Table 4 Average binding free energy values used to score the synthetic peptides (in kcal mol^{-1}). A first subset was selected using the mean value first 35 ns of molecular dynamics and the ff94 parameterization. For this subset, 40 ns dynamics were considered and average binding free energy values for the last 10 ns were used to select the best three peptides

Peptide	FF94 (0–35 ns)		FF94 (30–40 ns)		FF99SB (30–40 ns)		FF03 (30–40 ns)	
	MMPBSA	MMGBSA	MMPBSA	MMGBSA	MMPBSA	MMGBSA	MMPBSA	MMGBSA
Bak	−66.09	−79.70	−60.21	−69.71	−56.55	−70.58	−76.95	−84.98
$Bak_{16}Aib_4$	−72.00	−84.96	−73.82	−86.62	−66.08	−79.79	−63.55	−71.83
$Bak_{16}Aib_3G$	−73.06	−86.07	−83.31	−97.43	−67.28	−77.90	−63.06	−73.85
$Bak_{14}Aib_4$	−54.20	−59.64	–	–	–	–	–	–
$Bak_{13}Aib_3G$	−61.28	−74.56	−73.04	−79.18	−67.66	−80.78	−55.93	−59.98
$Bak_{13}Aib_4$	−54.10	−63.09	–	–	–	–	–	–
$Bak_{14}Aib_3G$	−59.19	−69.95	–	–	–	–	–	–
$Bak_{14}Aib_4G$	−84.01	−101.35	−93.20	−110.88	−92.14	−109.73	−64.14	−74.52
$Bak_{14}Aib_5$	−67.99	−75.04	–	–	–	–	–	–
$Bak_{16}Aib_5G$	−75.24	−93.99	−87.97	−107.78	−81.03	−95.52	−65.01	−73.36
$Bak_{16}Aib_6$	−75.98	−90.54	−70.30	−84.45	−68.32	−78.14	−79.33	−99.00

select the best scored peptides. Within a given force field, peptide rankings obtained with MMPBSA or MMGBSA methodologies were very similar, despite MMGBSA values were all lower than the corresponding MMPBSA ones.

It is worth noting that rankings obtained from the ff94 and ff99SB molecular dynamics, either using MMPBSA or MMGBSA, lead to the same two best scored peptides: $Bak_{14}Aib_4G$ and $Bak_{16}Aib_5G$. In addition, the predicted absolute values for ΔG_b using both methodologies are similar for these two peptides and also for the wild type Bak peptide. With respect to the other four studied peptides, different ranking are obtained depending on the selected approximation. However, ff94 force field strengthens the differences between them. Indeed, predicted binding energies for the third and the fourth peptides in the ranking differ by 9 kcal mol^{-1} and the latter has a ΔG_b 20 kcal mol^{-1} lower than the wild-type Bak peptide. Otherwise, ff99sb force field predict similar binding affinities for all four peptides, within a range of 4 kcal mol^{-1} and negligible differences between the third and the fourth classified. Thus, to choose a third peptide for the final ranking, we decided to take into account the ff94 force field differences. Hence, $Bak_{16}Aib_3G$, which is predicted to have a binding energy around 11 kcal mol^{-1} lower than the wild type Bak peptide, for both ff94 and ff99SB forced fields.

As can be seen from Table 5, the inclusion of the entropic contribution to the binding free energy estimation does not change the above discussed conclusions: the relative order of the three selected peptides is preserved and all of them have better $\Delta G_{binding}$ values than the reference Bak peptide.

As expected, the basic interaction pattern of all the selected peptides is very similar to the one of the Bak_{16} reference peptide (see Fig. 3 and Table S.8 of supporting information).

It is worth noting that the whole set of best scored peptides preserve Gly82, a residue experimentally reported as determinant for peptide activity.

Structural analysis

Helicity of BH3 only proteins has often been related to their binding affinity for the Bcl-x_L protein. Thus, helical properties of wild type Bak and best scored synthetic peptides in their bounded states were analyzed in order to determine if conformational space explored by these peptides can be related in any way with their predicted binding affinity (see Fig. 4 for helix propensity, Fig. 5 for helix ratio and Fig. 6 for helix residue length).

When comparing helical properties of the original BakBH3 peptide in the complex simulations, a general trend is observed for the different force fields used: ff99SB helical content is bigger than ff94 and the latter, than ff03. However, despite ff99SB leads to the highest helical content, it is well-known that ff94 should correspond to the most helical

Table 5 Average binding free energy values for the last 10 ns for the reference Bak peptide and for the three best-scored peptides, with and without inclusion of the entropic contribution. Values, calculated using the ff99SB force field, are reported in kcal mol^{-1}

Peptide	FF99SB (30–40 ns)			
	PB	GB	PB+ΔS	GB+ΔS
Bak	−56.55	−70.58	−15.86	−29.89
$Bak_{16}Aib_3G$	−67.28	−77.90	−25.11	−35.73
$Bak_{14}Aib_4G$	−92.14	−109.73	−56.23	−73.82
$Bak_{16}Aib_5G$	−81.03	−95.52	−41.72	−56.21

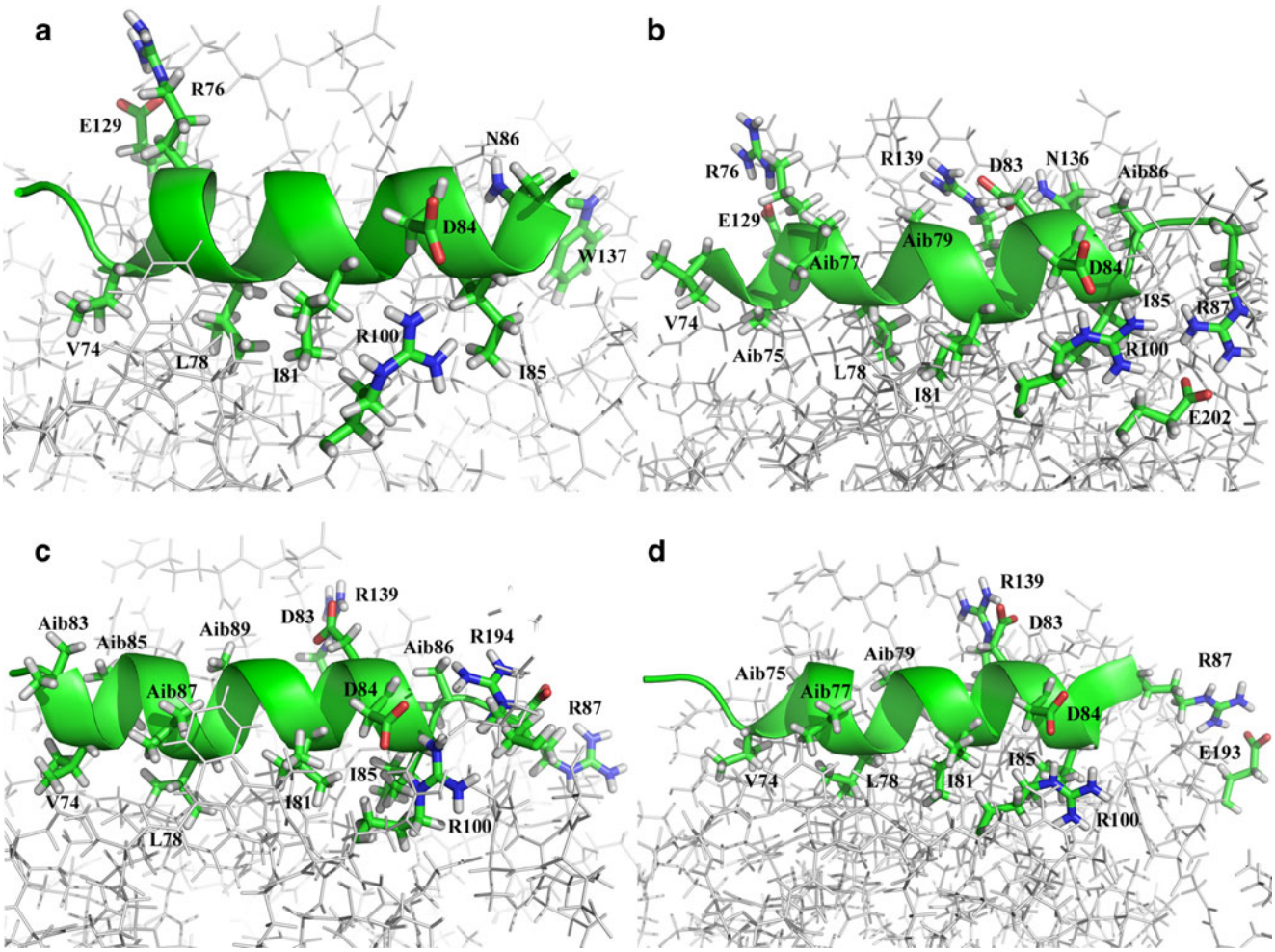

Fig. 3 Interaction pattern for (**a**) Bak_{16}, **b**) $Bak_{14}Aib_4G$, **c**) Bak16Aib5G and **d**) $Bak_{16}Aib_3G$ complexes

inducing parameterization. This trend cannot be clearly observed in helical propensity analysis for the other BH3 peptides. Omitting natural BakBH3 peptide, similar values are predicted for ff94 and ff99SB, both lead to a higher helical content than the ff03 parameterization. However, force field helical inducing effects are peptide dependent and no general trend can be elucidated from the parameterization used. Nonetheless, for ff94 and ff99SB force fields, peptide residues with a given helical tendency seem to be induced to adopt a helical conformation and all of them exhibit helical propensity values near the unity. Only those residues with clear non-helical conformations have low helical propensity values but

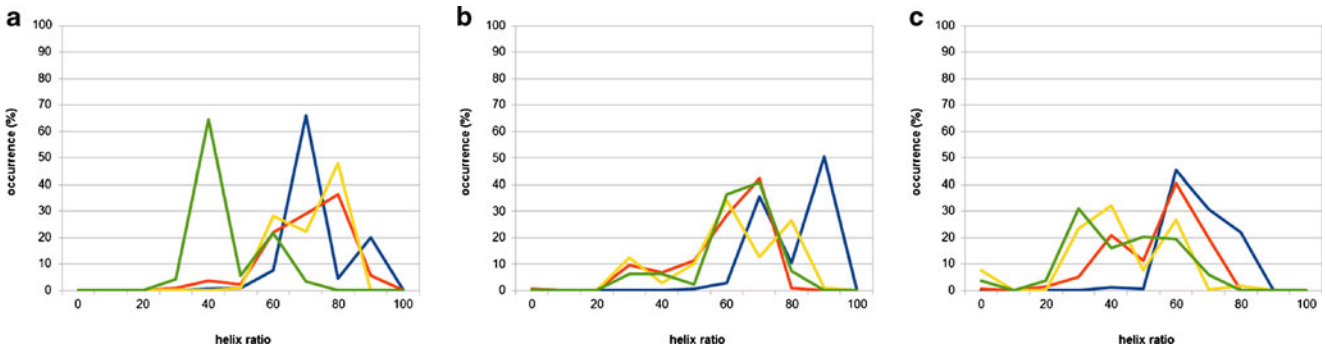

Fig. 4 Helical propensity values corresponding to the wild type Bak peptide (*on dark blue*) and the best scored synthetic peptides $Bak_{16}Aib_3G$, $Bak_{14}Aib_4G$ and $Bak_{16}Aib_5G$ (*on orange*, *yellow* and *green*, respectively) for the three force fields used: **a**) ff94; **b**) ff99SB; and **c**) ff03

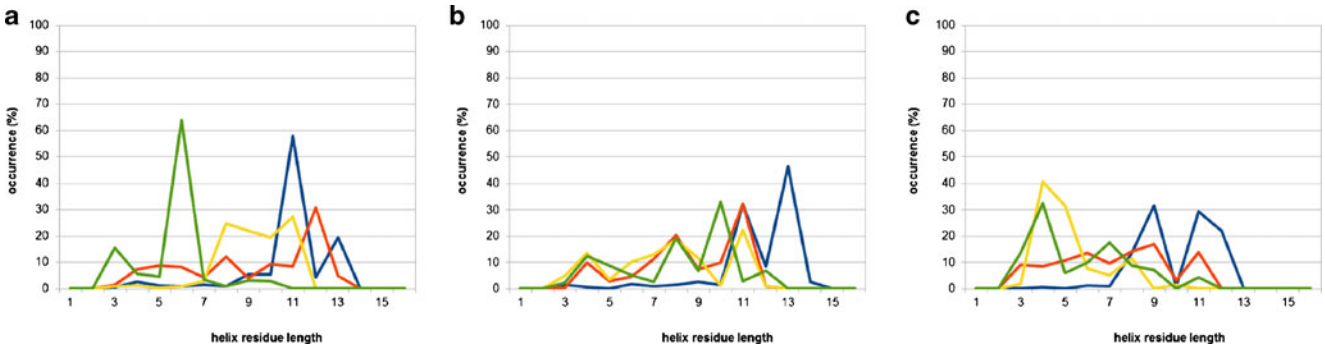

Fig. 5 Helix ratio values corresponding to the wild type Bak peptide (*on dark blue*) and the best scored synthetic peptides $Bak_{16}Aib_3G$, $Bak_{14}Aib_4G$ and $Bak_{16}Aib_5G$ (*on orange*, *yellow* and *green*, respectively) for the three force fields used: **a**) ff94; **b**) ff99SB; and **c**) ff03

halfway values are sparse. The opposite situation is found for ff03 force field. In this case, only residues with a clear helical conformation exhibit high helical content whereas the helical propensity values predicted for the major part of peptide residues are relatively low. However, it is worth noting that, despite being the less helical forming parameterization, ff03 exhibits some rare helical propensity trend in terminal regions. This fact was also observed in Fig. 2 where the C-terminal region of Bcl-x_L forms a small helical domain, not present in the remaining simulations. The more reliable situation seems to correspond to ff99SB, which exhibits intermediate values resulting from unbiased peptide conformations. These intermediate values are finally reflected into a higher overall helical content. Helix ratio and residue length also follows the above mentioned tendency for helical content. Accordingly, shorter helical preferences are observed for the ff03 than for ff94, the latter and ff99SB.

Regarding to differences in the peptides structure, no clear trends can be observed for the Aib helical induction. Surprisingly, for all force fields, wild type Bak peptide presents the highest helical properties content albeit Aib substitutions should favor helical conformations. Due to long simulation times required for structural rearrangements in modeled complexes, it can be thought that this low helical content may arise from unconverged simulations. However, binding free energy values and helical residues (values not shown) analyzed for the whole molecular dynamics trajectories reflect clearly converged simulations during the last 5 ns. Thus, this helical preference exhibited by wild-type Bak may be attributed to natural optimization of peptide structure. When introducing synthetic residues in peptide sequence, bonded peptide conformation has not necessarily to be identical to original peptide. In fact, optimal conformation for these new sequences seems to have a lower helical content. Thus, well known preference for helical conformations introduced by Aib mutations does not seem to be observed in bonded peptide conformations as protein environment hinders force field effects.

It has been reported that helical content of BH3 only proteins is strongly related to their binding affinities. Nonetheless, in the previously discussed results, no correlation was observed for any of the force field parameterizations considered. Thus, this increased binding affinity attributed to more helical peptides only makes sense from the point of view of the ratio of peptide bioactive conformation found in solution which is assumed to be helical.

Evolution of α-helical residues in BH3 free peptides simulations clearly reflect the helical inducing effects attributed to Aib residues (Fig. 7). As expected, all synthetic peptides, which contain Aib mutations, exhibit a higher helical content than wild-type Bak peptide. Free peptide conformations seem to converge after 50 ns of simulation, partially losing the initial helical domain. Wild-type Bak seems to completely lose its helical structure to explore different random coil conformations. Contrarily, Aib containing peptides preserve some kind

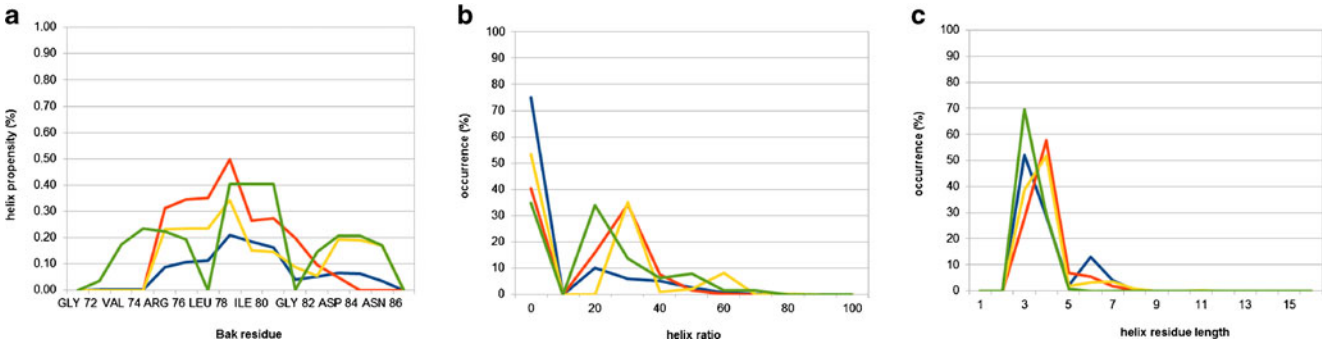

Fig. 6 Residue length values corresponding to the wild type Bak peptide (*on dark blue*) and the best scored synthetic peptides $Bak_{16}Aib_3G$, $Bak_{14}Aib_4G$ and $Bak_{16}Aib_5G$ (*on orange*, *yellow* and *green*, respectively) for the three force fields used: **a**) ff94; **b**) ff99SB; and **c**) ff03

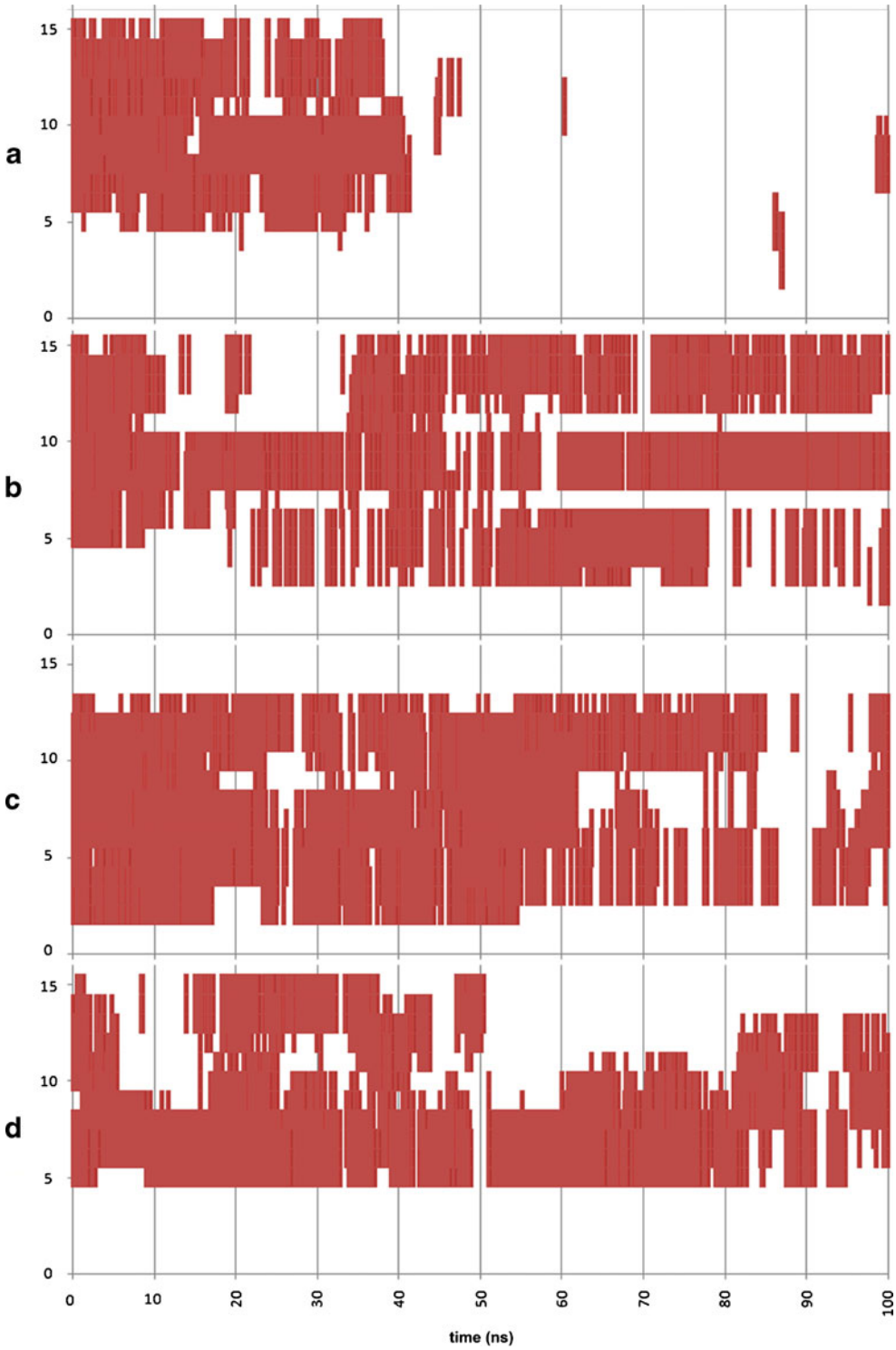

Fig. 7 α-helix secondary structure evolution of BH3 free peptides as evaluated by DSSP during the entire course of 100 ns MD simulation with ff99SB force field. **a** wild type Bak peptide, (**b**) $Bak_{16}Aib_5G$, (**c**) $Bak_{14}Aib_4G$ and (**d**) $Bak_{16}Aib_3G$

of helical structure during the whole molecular dynamics trajectory. Concretely, $Bak_{16}Aib_3G$ and $Bak_{14}Aib_4G$ prefer a bihelical conformation whereas in the $Bak_{16}Aib_5G$ peptide, the initial helical domain is broken into three helical fragments.

To quantify real differences in helical content of free peptides, for the last 25 ns, average properties were calculated (see Fig. 8). In comparison with bonded conformation, a considerable loss of helical content is observed similar for all peptides but wild-type Bak which does not contain Aib. Focusing on helical propensity, similar values are observed for synthetic peptides and the above mentioned trends to split the initial helical domain into smaller fragments can also be observed. From predicted values, $Bak_{14}Aib_4G$ seems to be the most helical peptide. When considering the helix ratio

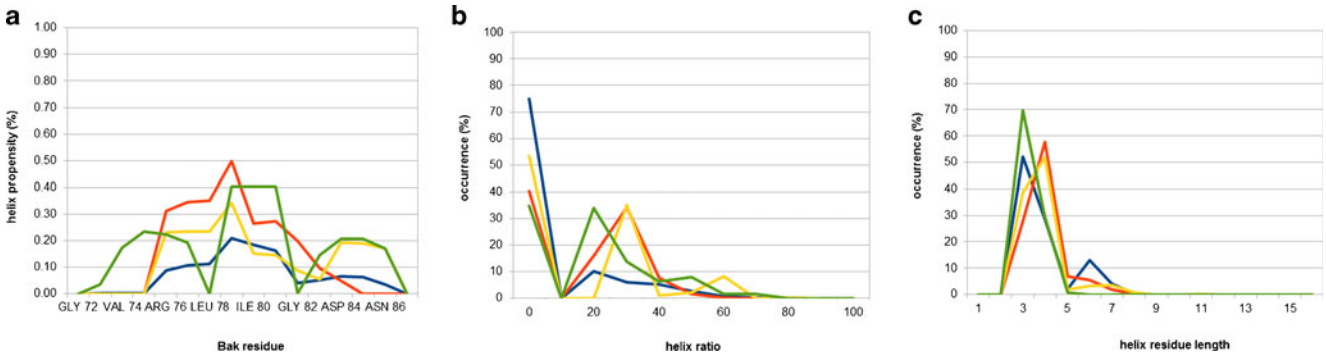

Fig. 8 Helical propensity, helix ratio and helix residue length values during the last 25 ns of MD simulations with ff99SB force field for BH3 free peptides. Wild type Bak peptide (*dark blue*), $Bak_{16}Aib_3G$ (*orange*), $Bak_{14}Aib_4G$ (*yellow*) and $Bak_{16}Aib_5G$ (*green*)

values, natural Bak appears again as the less helical peptide and a similar behavior is observed for the remaining synthetic peptides, only a bit lower for $Bak_{16}Aib_5G$. The analysis of the helix residue length clearly shows a preference for shorter helical segments in Aib containing peptides, only wild-type Bak has certain tendency to form larger helices. This fact is in good agreement with the split helical segments observed for Aib peptides.

In conclusion, it can be said that the force field parameterization used clearly bias conformational space explored by peptide residues. Nevertheless, helical properties of analyzed bonded peptides do not seem to be determinant in predicted binding affinities. Increased binding affinities observed experimentally for more helical peptides are only due to a higher ratio of bioactive peptide conformation in solution but not in bonded conformation.

Conclusions

Several authors report that an increase of the helical content of BH3 mimetic peptides considerably improves their binding affinity. In this context, this work aims at designing peptides derived from the BH3 domain of the proapoptotic protein Bak by substitution of some non-interacting residues by the helical inducing residue Aib. To this purpose, molecular dynamics were used to simulate wild type BakBH3 and proposed synthetic peptides. As the parameterization used seems to bias conformational space explored by the systems, different widely used force field were considered for simulations of these systems. The MM-PB/GBSA methodology was used to estimate binding affinities and the DSSP algorithm of Kabsch and Sander was used for analyzing the helical content.

As was expected, conformational space explored by the BakBH3/Bcl-x_L complex depended on the different force fields used. In agreement with parameterizations considered, it was observed that the ff03 behavior was different to the other parameterizations. As it should be expected, ff94 and ff99SB simulations lead to similar results, as ff99SB is just a correction of some ff94 parameters.

These differences observed in the conformational space explored by the complex were also reflected in a different interaction profile for the BakBH3 peptide. In this case, ff94 and ff99SB reproduced experimentally observed interactions but not, the ff03 results. It can be concluded that ff03 parameterization does not adequately describe this system as even starting from an experimental structure, it is not able to reproduce experimental interactions.

Designing peptides that preserve these well-known interactions for Bak BH3 domain and present an increased helical propensity should lead to a highest binding affinity for the Bcl-XL protein. However, it is noticeable that, in simulation of BH3 peptides complexes, does not exist a correlation between helical content and binding affinity. In addition, simulations of peptide complexes do not allow observing helical inducing effects of Aib due to the protein environment. Indeed, natural BakBH3 peptide presents the highest helical content but not the highest predicted binding affinity.

Free peptide simulations were also performed to observe the so-known Aib helical forming effects. These simulations clearly reflect an increase of helical content in synthetic peptides in comparison with natural BakBH3. As Aib substitutions do not affect BakBH3 residues relevant for binding, these peptides preserve relevant BakBH3 interactions (MM-GBSA per residue results not shown for synthetic peptides). In addition, this increased helicity leads to a higher ratio of bioactive conformation in solution, which is assumed to be helical, available to bind into the protein groove. Thus, proposed synthetic peptides should, a priori, exhibit a better binding affinity for Bcl-$_L$ with respect to natural BakBH3 peptide.

Finally, it is worth noting that the real efficiency of the proposed peptides should depend on other properties or interactions that were not included in the present study, due to its complexity. Additional interactions as aggregation of these proteins could also affect the binding of these proteins. Unfortunately, at the end, experiment is the only way to determine real peptide affinity.

References

1. J-j L, Lin M, J-y Y, Liu B, J-k B (2011) Targeting apoptotic and autophagic pathways for cancer therapeutics. Cancer Lett 300(2):105–114
2. Pavet V, Portal MM, Moulin JC, Herbrecht R, Gronemeyer H (2011) Towards novel paradigms for cancer therapy. Oncogene 30(1):1–20
3. Brenner D, Mak TW (2009) Mitochondrial cell death effectors. Curr Opin Cell Biol 21(6):871–877. doi:1016/j.ceb.2009.09.004
4. Tan M, Ooi J, Ismail N, Moad A, Muhammad T (2009) Programmed cell death pathways and current antitumor targets. Pharm Res 26(7):1547–1560. doi:10.1007/s11095-009-9895-1
5. Chipuk JE, Moldoveanu T, Llambi F, Parsons MJ, Green DR (2010) The BCL-2 family reunion. Mol Cell 37(3):299–310
6. Patel MP, Masood A, Patel PS, Chanan-Khan AA (2009) Targeting the Bcl-2. Curr Opin Oncol 21(6):516–523. doi:10.1097/CCO.0b013e328331a7a4
7. Richardson A, Kaye SB (2008) Pharmacological inhibition of the Bcl-2 family of apoptosis regulators as cancer therapy. Curr Mol Pharmacol 1(3):244–254
8. Day CL, Smits C, Fan FC, Lee EF, Fairlie WD, Hinds MG (2008) Structure of the BH3 domains from the p53-Inducible BH3-Only proteins Noxa and Puma in complex with Mcl-1. J Mol Biol 380(5):958–971
9. Lomonosova E, Chinnadurai G (2008) BH3-only proteins in apoptosis and beyond: an overview. Oncogene 27(Suppl 1):S2–19. doi:10.1038/onc.2009.39
10. Dutta S, Gullá S, Chen TS, Fire E, Grant RA, Keating AE (2010) Determinants of BH3 binding specificity for Mcl-1 versus Bcl-xL. J Mol Biol 398(5):747–762
11. Kazi A, Sun J, Doi K, Sung S-S, Takahashi Y, Yin H, Rodriguez J, Becerril J, Berndt N, Hamilton AD, Wang H-G, Sebti SM (2010) The BH3 α-helical mimic BH3-M6 disrupts BCL-XL, BCL-2 and MCL-1 protein-protein interactions with BAX, BAK, BAD or BIM and induces apoptosis in a BAX- and BIM-dependent manner. J Biol Chem. doi:10.1074/jbc.M110.203638
12. Shangary S, Oliver CL, Tillman TS, Cascio M, Johnson DE (2004) Sequence and helicity requirements for the proapoptotic activity of Bax BH3 peptides. Mol Cancer Ther 3(11):1343–1354
13. Liu D, Yang B, Cao R, Huang Z (2005) A chemical strategy to promote helical peptide-protein interactions involved in apoptosis. Bioorg Med Chem Lett 15(20):4467–4469. doi:10.1016/j.bmcl.2005.07.031
14. Petros AM, Nettesheim DG, Wang Y, Olejniczak ET, Meadows RP, Mack J, Swift K, Matayoshi ED, Zhang H, Fesik SW, Thompson CB (2000) Rationale for Bcl-XL/Bad peptide complex formation from structure, mutagenesis, and biophysical studies. Protein Sci 9(12):2528–2534. doi:10.1110/ps.9.12.2528
15. Yang B, Liu D, Huang Z (2004) Synthesis and helical structure of lactam bridged BH3 peptides derived from pro-apoptotic Bcl-2 family proteins. Bioorg Med Chem Lett 14(6):1403–1406. doi:10.1016/j.bmcl.2003.09.101
16. Yang C-Y, Nikolovska-Coleska Z, Li P, Roller P, Wang S (2004) Solution conformations of wild-type and mutated bak BH3 peptides via dynamical conformational sampling and implication to their binding to antiapoptotic Bcl-2 proteins. J Phys Chem B 108(4):1467–1477. doi:10.1021/jp036009f
17. Lama D, Sankararamakrishnan R (2011) Molecular dynamics simulations of pro-apoptotic BH3 peptide helices in aqueous medium: relationship between helix stability and their binding affinities to the anti-apoptotic protein Bcl-XL. J Comput Aided Mol Des 25(5):413–426. doi:10.1007/s10822-011-9428-y
18. Modi V, Lama D, Sankararamakrishnan R (2013) Relationship between helix stability and binding affinities: molecular dynamics simulations of Bfl-1/A1-binding pro-apoptotic BH3 peptide helices in explicit solvent. J Biomol Struct Dyn 31(1):65–77. doi:10.1080/07391102.2012.691363
19. Marshall GR, Hodgkin EE, Langs DA, Smith GD, Zabrocki J, Leplawy MT (1990) Factors governing helical preference of peptides containing multiple alpha, alpha-dialkyl amino acids. Proc Natl Acad Sci U S A 87(1):487–491
20. Toniolo C, Bonora GM, Bavoso A, Benedetti E, di Blasio B, Pavone V, Pedone C (1983) Preferred conformations of peptides containing α, α-disubstituted α-amino acids. Biopolymers 22(1):205–215. doi:10.1002/bip.360220129
21. Basu G, Kuki A (1992) Conformational preferences of oligopeptides rich in alpha-aminoisobutyric acid. II. A model for the 3(10)/alpha-helix transition with composition and sequence sensitivity. Biopolymers 32(1):61–71. doi:10.1002/bip.360320109
22. Cornell WD, Cieplak P, Bayly CI, Gould IR, Merz KM, Ferguson DM, Spellmeyer DC, Fox T, Caldwell JW, Kollman PA (1995) A second generation force field for the simulation of proteins, nucleic acids, and organic molecules. J Am Chem Soc 117(19):5179–5197. doi:10.1021/ja00124a002
23. Case D, Darden T, Cheatham III T, Simmerling C, Wang J, Duke R, Luo R, Merz K, Pearlman D, Crowley M, Walker R, Zhang W, Wang B, Hayik S, Roitberg A, Seabra G, Wong K, Paesani F, Wu X, Brozell S, Tsui V, Gohlke H, Yang L, Tan C, Mongan J, Hornak V, Cui G, Beroza P, Mathews D, Schafmeister C, Ross W, Kollman P (2006) AMBER 9. University of California, San Francisco
24. Case DA, Cheatham TE 3rd, Darden T, Gohlke H, Luo R, Merz KM Jr, Onufriev A, Simmerling C, Wang B, Woods RJ (2005) The Amber biomolecular simulation programs. J Comput Chem 26(16):1668–1688. doi:10.1002/jcc.20290
25. Kollman PA, Dixon R, Cornell W, Fox T, Chipot C, Pohorille A (1997) The development/application of a minimalist molecular mechanics force field using a combination of ab initio calculations and experimental data. In: van Gunsteren W, Wilkinson A, Weiner P (eds) Computer simulations of biomolecular systems, vol 3, Kluwer, Dordrecht, The Netherlands, pp 83–96
26. Hornak V, Abel R, Okur A, Strockbine B, Roitberg A, Simmerling C (2006) Comparison of multiple Amber force fields and development of improved protein backbone parameters. Proteins 65(3):712–725. doi:10.1002/prot.21123
27. Duan Y, Wu C, Chowdhury S, Lee MC, Xiong G, Zhang W, Yang R, Cieplak P, Luo R, Lee T, Caldwell J, Wang J, Kollman P (2003) A point-charge force field for molecular mechanics simulations of proteins based on condensed-phase quantum mechanical calculations. J Comput Chem 24(16):1999–2012. doi:10.1002/jcc.10349
28. Sattler M, Liang H, Nettesheim D, Meadows RP, Harlan JE, Eberstadt M, Yoon HS, Shuker SB, Chang BS, Minn AJ, Thompson CB, Fesik SW (1997) Structure of Bcl-xL-Bak peptide complex: recognition between regulators of apoptosis. Science 275(5302):983–986
29. Jorgensen WL, Chandrasekhar J, Madura JD, Impey RW, Klein ML (1983) Comparison of simple potential functions for simulating liquid water. J Chem Phys 79(2):926–935
30. Bisetty K, Gomez-Catalan J, Aleman C, Giralt E, Kruger HG, Perez JJ (2004) Computational study of the conformational preferences of the (R)-8-amino-pentacyclo[5.4.0.0(2,6).0(3,10).0(5,9)]undecane-8-carboxylic acid monopeptide. J Pept Sci 10(5):274–284. doi:10.1002/psc.526
31. Berendsen HJC, Postma JPM, Gunsteren WF, DiNola A, Haak JR (1984) Molecular dynamics with coupling to an external bath. J Chem Phys 81(8):3684–3690
32. Darden T, York D, Pedersen L (1993) Particle mesh Ewald: an N log(N) method for Ewald sums in large systems. J Chem Phys 98(12):10089–10092
33. Ryckaert J-P, Ciccotti G, Berendsen HJC (1977) Numerical integration of the cartesian equations of motion of a system with constraints: molecular dynamics of n-alkanes. J Comput Phys 23(3):327–341
34. Srinivasan J, Cheatham TE, Cieplak P, Kollman PA, Case DA (1998) Continuum Solvent Studies of the Stability of DNA, RNA, and

Phosphoramidateâ'DNA Helices. J Am Chem Soc 120(37):9401–9409. doi:10.1021/ja981844+
35. Kollman PA, Massova I, Reyes C, Kuhn B, Huo S, Chong L, Lee M, Lee T, Duan Y, Wang W, Donini O, Cieplak P, Srinivasan J, Case DA, Cheatham TE 3rd (2000) Calculating structures and free energies of complex molecules: combining molecular mechanics and continuum models. Acc Chem Res 33(12):889–897. doi:10.1021/ar000033j
36. Luo R, David L, Gilson MK (2002) Accelerated Poisson-Boltzmann calculations for static and dynamic systems. J Comput Chem 23(13):1244–1253. doi:10.1002/jcc.10120
37. Lamm G (2003) The Poisson–Boltzmann equation. Reviews in computational chemistry. Wiley, New York doi:10.1002/0471466638.ch4
38. Baker NA (2005) Biomolecular applications of Poisson–Boltzmann methods. Reviews in computational chemistry. Wiley, New York doi:10.1002/0471720895.ch5
39. Tsui V, Case DA (2000) Theory and applications of the generalized born solvation model in macromolecular simulations. Biopolymers 56(4):275–291
40. Weiser J, Shenkin PS, Still WC (1999) Approximate atomic surfaces from linear combinations of pairwise overlaps (LCPO). J Comput Chem 20(2):217–230
41. Sitkoff D, Sharp KA, Honig B (1994) Accurate calculation of hydration free energies using macroscopic solvent models. J Phys Chem 98(7):1978–1988
42. Gohlke H, Kiel C, Case DA (2003) Insights into protein-protein binding by binding free energy calculation and free energy decomposition for the Ras-Raf and Ras-RalGDS complexes. J Mol Biol 330(4):891–913
43. Kabsch W, Sander C (1983) Dictionary of protein secondary structure: pattern recognition of hydrogen-bonded and geometrical features. Biopolymers 22(12):2577–2637. doi:10.1002/bip.360221211
44. Lama D, Sankararamakrishnan R (2008) Anti-apoptotic Bcl-XL protein in complex with BH3 peptides of pro-apoptotic Bak, Bad, and Bim proteins: comparative molecular dynamics simulations. Proteins 73(2):492–514. doi:10.1002/prot.22075